



## COVER SHEET

---

**This is the author-version of article published as:**

Frost, Ray and Palmer, Sara and Reddy, Jagannadha (2007) Application of UV-Vis, near-infrared and mid-infrared spectroscopy to the study of Mn-bearing humites. *Polyhedron* 26(2):pp. 524-533.

Accessed from <http://eprints.qut.edu.au>

Copyright 2007 Elsevier

# Application of UV-Vis, near-infrared and mid-infrared spectroscopy to the study of Mn-bearing humites

Sara Palmer, B. Jagannadha Reddy, Ray L. Frost\*

*Inorganic Materials Research Program, School of Physical and Chemical Sciences, Queensland University of Technology, GPO Box 2434, Brisbane Queensland 4001, Australia*

## Abstract

The combination of electronic and vibrational spectra has been applied to correlate the spectral properties, with composition, structure and cation substitutions such as Mn, Fe, Ca and Zn for Mg in humites: norbergite, alleghanyite, leucophoenicite and sonolite with increasing number of silicate layers, 1, 2, 3 and 4. The observation of two broad bands in the visible range, near 550 nm and 450 nm ( $18180$  and  $22220\text{ cm}^{-1}$ ) and one sharp band around 410 nm ( $24390\text{ cm}^{-1}$ ) is characteristic of  $\text{Mn}^{2+}$  in alleghanyite and leucophoenicite. The study of UV-Vis (electronic) spectral features confirms Mn as a major substituent in these two samples. Cation impurities like Zn and Ca as revealed from EDX analysis might be the cause for the absence of Mn-type spectrum in sonolite. The first observation is the near-infrared spectra of all four minerals in the first fundamental overtone OH-stretching mode are different and each mineral is characterized by its NIR spectrum. The feature in the range  $7180\text{--}6600\text{ cm}^{-1}$  [ $1393$  to  $1515\text{ nm}$  or  $1.39$  to  $1.52\text{ }\mu\text{m}$ ] corresponds to the overtones of OH stretching vibrational modes of the humite groups observed in their IR spectra over the range,  $3680\text{--}3320\text{ cm}^{-1}$ . The infrared spectra of the hydrous components of OH and  $\text{SiO}_4$  groups in the mineral structure act as an aid to distinguish the minerals of the humite mineral group. A band at  $541\text{ cm}^{-1}$  is assigned to MnO stretching mode.

*Key words:* Norbergite; Alleghanyite; Leucophoenicite; Sonolite, UV-Vis, NIR and mid-IR spectroscopy; Electronic spectra of  $\text{Mn}^{2+}$ ; Overtone and combination bands; Layered silicates

---

\* Author to whom correspondence should be addressed (r.frost@qut.edu.au)

## 1. Introduction

The humite minerals have been studied for almost 100 years [1-9]. Crystal structures were elucidated in the 1960's and 1970's [10-21]. The minerals are structurally analogous to olivine [22]. Much variation in the composition of the minerals is observed due to isomorphic substitution [22]. Many of the minerals contain manganese as the substituent [22-25]. No near-infrared spectroscopic studies of the minerals have been forthcoming. The humite minerals are a group of four homologues that are represented by the general formula  $n\text{Mg}_2\text{SiO}_4 \cdot \text{Mg}(\text{OH},\text{F})_2$  where  $n = 1$  for norbergite,  $n = 2$  for chondrodite,  $n = 3$  for humite and  $n = 4$  for clinohumite [26]. The humite group of minerals forms a morphotropic series with the mineral olivine and brucite. The members of this group differ not only by chemistry but by the number of olivine or silicate layers that are present between the brucite layers. There can be either one, two, three or four layers of the silicate layers between each brucite-like sheet. This has the effect of extending the unit cell of the minerals and affecting their symmetries.

The humite minerals are a homologous series of magnesium-ferrous-manganese orthosilicates whose structures are based on hexagonal closest-packed arrays of anions (O,F,OH) with octahedral and tetrahedral cation distributions related to that in forsterite. In humite there are 4 distinct octahedra; M(1)O6 and M(2)O6, like those in olivine, and M(2)O5(F,OH)1 and M(3)O4(F,OH)2, like those in chondrodite. Ferrous Fe is ordered in equal amounts (approximately 0.1  $\text{Fe}^{2+}$ ) into the more distorted octahedra with 6 O ligands but avoids the less distorted octahedra with 1 or 2 (F,OH) ligands. In these closely packed orthosilicates, all anions are charge-balanced, and  $\text{Fe}^{2+}$  prefers the more distorted sites than those with the more polarizable ligands. In Mg/Fe olivines the M(1)O6 octahedron is significantly smaller but slightly more distorted than M(2)O6. A general mineralogy, chemistry and crystal structures of the humite series and Mn-analogs have been well-studied and summarized by Ribbe [18, 22, 28]. A recent study of the structure of a natural chondrodite by neutron diffraction demonstrated that hydrogen is found to occupy the H1 site. The significance of hydrogen-bonding has been explained in humite structures containing varying amounts of OH, F and Ti [6]. A few spectroscopic studies are made on humite [29, 30] and iron-rich clinohumites [31]. There are many studies reported on the vibrational modes of olivines by infrared and Raman spectroscopy [10-16].

Humites may contain Mg, Ca, Ti, Mn, Fe and Zn although only Mg, Mn and Ca form end members. These cations are ordered into the octahedral sites which vary in distortion, ligancy, size, and symmetry. A better understanding of the behaviour of cations substitution for Mg in humites is expected to provide a helpful guidance for spectral analysis of Mn-bearing minerals. It is our intention that makes the study of manganese humites and to compare with the Mg bearing humite.

Norbergite,  $\text{Mg}_3(\text{SiO}_4)(\text{OH}, \text{F})_2$  is a member of humite group. Humite group minerals possess silicate layers and oxide layers in their structures. The silicate layers and oxide layers have the same structure as olivine and brucite respectively. The Raman spectra of norbergite samples were investigated and explained the dependence of OH Raman bands on temperature and pressure [32]. The magnesium humites (norbergite, chondrodite, humite and clinohumite) have been studied and summerised [33]. Their manganese analogues (alleghanyite, leucophoenicite, sonalite,

jerrygibbsite, ribbeite and manganhumite) have received less attention. They are, in general, less common, found in metamorphosed Mn-deposits. Alleghanyite,  $Mn_5(SiO_4)(OH)_2$  species crystal structure was reported by Rentzeperis [34], a high Mg alleghanyite from Sterling Hill was described by Petersen et al. [35] and later crystal structure refinement report [36] shows cations in alleghanyite and all other humite group minerals are ordered in octahedral sites accordingly to size criteria, eventhough ligancy (O, OH, F) may be the controlling factor where charge balance and crystal-field effects are involved. Penfield and Warren [37] disclosed originally the mineral, leucophoenicite,  $(Mn^{2+})_7(SiO_4)_3(OH)_2$  and its crystal structure solved by Moore [38,39] confirms edge-sharing, half-occupied, silicate tetrahedra and is structurally distinct from the humite group minerals. Later, the study of TEM images of leucophoenicite [40], supports the structure analysis done by Moore's structural report [38]. Sonlitnolite,  $Mn^{2+}_9(SiO_4)_4(OH)_2$  was first described by Yoshinaga [41]. from eleven localities in Japan and crystal structure was discussed by Ribbe [33].

The expression of Mn humite minerals, their formula, number of silicate layers and symmetry class are described in Table 1. Previous studies have been based on the chemistry and structural analysis. No spectroscopic studies were included in previous research and this is why we are presenting this work. In this communication, we present the spectroscopic investigations of selected manganese humites (alleghanyite, leucophoenicite, sonalite) and Mg-humite for comparison.

## 2. Experimental

### 2.1. Minerals

The minerals used in this work listed in Table 1 were obtained on loan from The South Australian Museum and from the Mineralogical Research Company. The minerals have been analysed by X-ray diffraction for phase identification and by SEM together with electron probe analysis for chemical composition.

### 2.2. SEM and EDX analysis

For X-ray microanalysis (EDX), samples were embedded in araldite resin and polished with diamond paste on Lamplan 450 polishing cloth using water as a lubricant. Next, the samples were coated with a thin layer of evaporated carbon for conduction and examined in a JEOL 840A analytical SEM (JEOL Ltd, Tokyo, Japan) at 25kV accelerating voltage. Preliminary analyses of the humite mineral samples were carried out on the FEI Quanta SEM using an EDAX microanalyser (FEI Company, Hillsboro, Oregon, USA), and microanalysis of the clusters of fine crystals was carried out using a full standards quantitative procedure on the JEOL 840 SEM using a Moran Scientific microanalysis system (Tokyo, Japan). Oxygen was not measured directly but calculated using assumed stoichiometries to the other elements analysed.

### 2.3. UV-Vis spectroscopy

UV-Visible spectrophotometer (Varian Cary 3, Melbourne, Australia), equipped with a Diffuse Reflectance Accessory (DRA) was employed to record the electronic spectra of the samples in the region between 200 and 900 nm ( $50,000$  to  $11110\text{ cm}^{-1}$ ). This technique allows the study of the reflectance spectra of the samples

in the powder form. The DRA consists of a 73 mm diameter integrating sphere, featuring an inbuilt high performance photomultiplier. Sample was mounted on coarse filter paper by resuspending the sample and submerging the filter paper into the suspension. Initially a base line was recorded using two pressed polytetrafluoroethylene (PTFE) reference disks. Next, the sample was mounted flat over the sample port and the reflectance spectrum of the sample, relative to the reference disks, was collected by the integrating sphere. By placing the sample flat any specular components of reflectance should be directed out of the DRA entrance port, as the angle of incidence is  $0^{\circ}$ . The diffuse reflectance measurements were converted into absorption (arbitrary units) using the Kubelka-Munk function. Data manipulation was performed using Microsoft Excel.

#### 2.4. NIR and Infrared Spectroscopy

NIR spectra were collected on a Nicolet Nexus FT-IR spectrometer with a Nicolet Near-IR Fibreport accessory in diffuse reflectance mode. A white light source was used, with a quartz beam splitter and TEC NIR InGaAs detector. Spectra were obtained from 11 000 to 4000  $\text{cm}^{-1}$  (909 – 2,500 nm) by the co-addition of 64 scans at a resolution of 8  $\text{cm}^{-1}$ . A mirror velocity of 1.2659 m/s was used. The spectra were transformed using the Kubelka-Munk algorithm ( $f(R_{\infty}) = (1 - R_{\infty})^2/2R_{\infty}$ ) for comparison with absorption spectra.

Mid-infrared and NIR spectra were obtained using an FT spectrometer ((Nicolet Nexus, Madison, Wisconsin, USA) with a "smart endurance" single bounce diamond ATR cell. Spectra over the 4000 to 500  $\text{cm}^{-1}$  (2,500 – 20,000 nm) range were obtained by the co-addition of 64 scans with a resolution of 4  $\text{cm}^{-1}$  and a mirror velocity of 0.6329 cm/s.

The spectral manipulations of baseline adjustment, smoothing, and normalisation were performed using the Spectralcalc software package GRAMS (Galactic Industries Corporation, NH, USA). Band component analysis was carried out using peakfit software (Jandel Scientific, Postfach 4107, D-40688 Erkrath, Germany). Lorentz-Gauss cross product functions were used through out and peak fit analysis undertaken until squared correlation coefficients with  $R^2$  greater than  $>0.995$  were obtained.

### 3. Results and discussion

#### 3.1. SEM analysis

The EDX quantitative analyses were made on different areas of the samples. and selected one set of EDX spectra of humites studied in this work. The spectra were de-convoluted and calibrated to produce the chemical formula as given in Table 1. The analysis is in harmony with the accepted formula of humites. The data in the table shows Mg is major and Fe as minor impurity in norbergite where as other minerals are rich in manganese with minor inclusions of Mg, Ca, Zn and F. For sonalite, the chemical formula has been calculated from the analytical data reported for manganese humites, including sonalite originating from Franklin, New Jersey [42]. The sonolite mineral from the same origin is used in the present study.

### 3.2. UV-Vis (electronic) spectroscopy

For a given symmetry, transition metal ion can produce a characteristic absorption spectrum and spectra of minerals may be used to identify ions in unusual oxidation states and the symmetry of co-ordination states. The electronic spectra of iron group ions can be studied in the 200-900 nm region ( $50000-11110\text{ cm}^{-1}$ ). The valency of manganese is two in most of the minerals. The ground state for  $\text{Mn}^{2+}$  ( $d^5$ ) is  ${}^6\text{S}$  which transforms into  ${}^6\text{A}_{1g}$  in crystal field. The excited states of  $d^5$  ions are quartet ( ${}^4\text{G}$ ,  ${}^4\text{F}$ ,  ${}^4\text{D}$ ,  ${}^4\text{P}$ ) and doublet ( ${}^2\text{I}$ ,  ${}^2\text{H}$ ,  ${}^2\text{G}$ ,  ${}^2\text{F}$ ,  ${}^2\text{D}$ ,  ${}^2\text{P}$ ,  ${}^2\text{S}$ ) terms. Thus sextet-quartet/sextet-doublet transitions result for  $d^5$  ions and are called spin-forbidden transitions. Usually sextet-quartet transitions are observed and  $\text{Mn}^{2+}$  ion in octahedral coordination gives rise to two broad bands in the range 600- 450 nm ( $16665-22220\text{ cm}^{-1}$ ) and one sharp band around 400 nm ( $25000\text{ cm}^{-1}$ ) [43-45]. The study of UV-Vis spectroscopy of humites, reveals the electronic spectra for two samples, alleghanyite and leucophoenicite. It is not surprising to note the absence of a Mn-spectrum in norbergite since Mg is major cation. Whereas in sonolite the contribution by Mn is expected but surprisingly is absent in the spectrum. At least there are two reasons that can be reasonably accounted. The presence of Mn is very low when compared to the other two Mn-bearing humites. The other factor, for the suppression of the spectrum is due to the presence of cations like Zn and Ca. The contribution of cations, like Zn and Ca might be effective for masking the Mn-type spectrum in sonolite ( $\text{Mn}^{2+}_{0.9}\text{Zn}^{2+}_{0.06}\text{Ca}^{2+}_{0.03}(\text{SiO}_4)_4(\text{OH}_{0.56}\text{F}_{0.44})$ ).

The electronic spectra of the two bivalent Mn-minerals; alleghanyite,  $\text{Mn}_{11.48}(\text{SiO}_4)_2(\text{OH},\text{F})_{3.48}$  and leucophoenicite,  $\text{Mn}_{6.47}\text{Mg}_{0.19}\text{Ca}_{0.45}(\text{SiO}_4)_3(\text{OH})_{2.22}$  are shown in Fig. 1. The spectra of the two samples look alike but band positions differ only slightly. The observation of two broad bands in the visible range, near 550 nm and 450 nm ( $18180$  and  $22220\text{ cm}^{-1}$ ) and one very sharp band around 410 nm ( $24390\text{ cm}^{-1}$ ) are characteristic of  $\text{Mn}^{2+}$  in these minerals. The first broad feature observed at 549 nm ( $18215\text{ cm}^{-1}$ ) is attributed to  ${}^6\text{A}_{1g}(\text{S}) \rightarrow {}^4\text{T}_{1g}(\text{G})$  transition and a similar broad band but relatively less intense at 453 nm ( $22075\text{ cm}^{-1}$ ) is identified as  ${}^6\text{A}_{1g}(\text{S}) \rightarrow {}^4\text{T}_{2g}(\text{G})$  transition. These transitions are shifted for leucophoenicite, at 558 ( $17920\text{ cm}^{-1}$ ) and 441 nm ( $22675\text{ cm}^{-1}$ ) with additional shoulder at 435 nm ( $22990\text{ cm}^{-1}$ ). For Mn-rich mineral, sursasite, bands at 580 nm ( $17240\text{ cm}^{-1}$ ) and 515 nm ( $19420\text{ cm}^{-1}$ ) are assigned to  ${}^6\text{A}_{1g}(\text{S}) \rightarrow {}^4\text{T}_{1g}(\text{G})$  and  ${}^6\text{A}_{1g}(\text{S}) \rightarrow {}^4\text{T}_{2g}(\text{G})$  transition respectively [46].  ${}^4\text{A}_{1g}(\text{G})$  and  ${}^4\text{E}_{1g}(\text{G})$  states give rise to sharp bands because of these states are independent of crystal-field, Dq [47]. The sharp line like bands of alleghanyite in UV region at 413 nm ( $24210\text{ cm}^{-1}$ ) and 408 nm ( $24510\text{ cm}^{-1}$ ) are identified as independent crystal field transitions and are assigned to  ${}^6\text{A}_{1g}(\text{S}) \rightarrow {}^4\text{A}_{1g}(\text{G})$  and  ${}^6\text{A}_{1g}(\text{S}) \rightarrow {}^4\text{E}_{1g}(\text{G})$  transitions respectively. An almost a similar feature is seen for leucophoenicite. These bands are shifted to higher wavenumbers in the UV region.  $\text{Mn}^{2+}$  in silicate melts and glasses consist of a band at 415 nm ( $24095\text{ cm}^{-1}$ ) and explained the cause of this band by two transitions,  ${}^6\text{A}_{1g}(\text{S}) \rightarrow {}^4\text{A}_{1g}(\text{G})$  and  ${}^6\text{A}_{1g}(\text{S}) \rightarrow {}^4\text{E}_{1g}(\text{G})$  [48]. The observation of splitting for the UV band at around 410 nm ( $24390\text{ cm}^{-1}$ ) shows with distinguishable energy may be explained by the distortion of octahedral symmetry of  $\text{Mn}^{2+}$  ions in both the minerals. The assignment of the  $\text{Mn}^{2+}$  bands in humites are presented in Table 2 along with the bands reported for Mn-bearing silicate [46]. The variation in band positions with shifts to higher wavenumbers may be due to the presence of Mg and Ca in these minerals.

### 3.3. NIR spectroscopy

Near-infrared spectra of Mn-humite mineral group covering a wide range in composition show diagnostic absorption bands related to vibrational processes involving hydroxyl units. Many of these absorption bands are relatively broad and overlapping. However, by the application of spectral analysis methods like continuum removal and derivate analysis permit minerals (under study) to be distinguished. The main spectral differences between the minerals are illustrated in plots showing major absorption band centres and other spectral feature positions. The observed NIR spectral features may conveniently subdivide into three regions (Fig. 2 to 4): (a) the first region is the high wavenumber region  $7400\text{-}6400\text{ cm}^{-1}$  ( $1351\text{-}1562\text{ nm}$ ) ( $1.35\text{-}1.56\text{ }\mu\text{m}$ ) attributed to the OH stretching and bending modes (Fig. 2); (b) the  $5650\text{-}4650\text{ cm}^{-1}$  ( $1770\text{-}2150\text{ nm}$ ) ( $1.77\text{-}2.15\text{ }\mu\text{m}$ ) region attributed to combination of OH and Si-OH modes shown in Fig. 3 and (c) the  $4600\text{-}4000\text{ cm}^{-1}$  ( $2174\text{-}2500\text{ nm}$ ) ( $2.17\text{-}2.50\text{ }\mu\text{m}$ ) region assigned to the combination of the stretching and deformation modes of humite minerals and are related manganese(II) hydroxide and the spectra are shown in Fig. 4.

#### *The $7400\text{ to }6400\text{ cm}^{-1}$ ( $1351\text{-}1562\text{ nm}$ ) ( $1.35\text{-}1.56\text{ }\mu\text{m}$ ) spectral region*

In this spectral region where the first overtones of the OH stretching vibrations are shown for norbergite, alleghanyite, leucophoenicite and sonalite in Fig. 2. Norbergite, a single-layered silicate, shows unique spectrum at around  $7180\text{ cm}^{-1}$  and the spectrum is resolved into one sharp peak at  $7180\text{ cm}^{-1}$  ( $1393\text{ nm}$ ) ( $1.39\text{ }\mu\text{m}$ ) and two weak bands at  $7165$  and  $7035\text{ cm}^{-1}$  ( $1396$  and  $1422\text{ nm}$ ) ( $1.40$  and  $1.42\text{ }\mu\text{m}$ ). These bands are shifted to lower wavenumbers and appear with distorted modes for the 2-layered and 3-layered alleghanyite and leucophoenicite minerals respectively. It may also be explained that the possible substitutions of cations of Mn/Zn/Ca/Fe for Mg are responsible for the complexity of bands in their spectra. The spectrum is more complicated for the 4-layered sonalite and may be resolved into a series of overlapping bands. The first observation is the spectra of all the four minerals in the region  $7400\text{ to }6400\text{ cm}^{-1}$  ( $1351\text{ to }1562\text{ nm}$ ) ( $1.35\text{ to }1.56\text{ }\mu\text{m}$ ) are different and each mineral is characterized by NIR spectrum. Bands from  $7180\text{ to }6600\text{ cm}^{-1}$  ( $1393\text{ to }1515\text{ nm}$ ) ( $1.39\text{ to }1.52\text{ }\mu\text{m}$ ) correspond to the overtones of OH stretching vibrational modes of the humite groups shown in their IR spectra over the range,  $3680\text{-}3320\text{ cm}^{-1}$  (Fig. 4). Bands appear as shoulders to the higher wavenumbers of the sharp peak at  $7180\text{ cm}^{-1}$  ( $1393\text{ nm}$ ) ( $1.39\text{ }\mu\text{m}$ ) may be attributed to the combination of OH-stretching fundamental and MOH-deformation modes ( $2\times\text{OH}$  fundamental + OH deformation) [49]. These spectral features confirm range of compositional variations in humite group minerals. For example,  $M = \text{Mg}$  in sonalite, the weak shoulders at  $7205\text{ cm}^{-1}$  ( $1388\text{ nm}$ ) ( $1.39\text{ }\mu\text{m}$ )  $\text{cm}^{-1}$  might be the result of MgOH. The same band appears with variable band positions and intensity in other minerals. For alleghanyite, leucophoenicite and sonalite 'M' may be Mn/Ca/Zn that causes the change in intensity and positions of bands in the spectrum.

#### *The $5650\text{-}4650\text{ cm}^{-1}$ ( $1770\text{-}2150\text{ nm}$ ) ( $1.77\text{-}2.15\text{ }\mu\text{m}$ ) spectral region*

The 5650-4650  $\text{cm}^{-1}$  (1770-2150 nm) (1.77-2.15  $\mu\text{m}$ ) spectral region (Fig. 3) shows a number of vibrational modes. The broad spectrum centred at 5200  $\text{cm}^{-1}$  (1923 nm) (1.92  $\mu\text{m}$ ) is a common feature to the spectra of humites. Each spectrum is resolved into three peaks. The most pronounced band registered in all the spectra is near 5030  $\text{cm}^{-1}$  (1988 nm) (1.99  $\mu\text{m}$ ) is probably due to the combination of OH and Si-OH modes [50]. The observation of the most intense band for Fe-humites at 5200  $\text{cm}^{-1}$  (1923 nm) (1.92  $\mu\text{m}$ ) has been attributed to the combinational band of OH and Si-OH modes. For norbergite the main bands are located at 5240, 5165 and 5030  $\text{cm}^{-1}$  (1908, 1936 and 1988 nm) (1.91, 1.94 and 1.99  $\mu\text{m}$ ) and alleghanyite displays almost similar spectrum with a little/ minor variation of band positions. The intensity and position of the bands are variable in leucophoenicite and sonalite from one another. The complexity of bands increases with the order of silicate layers in humites. Thus Fig. 3 shows characteristic patterns due to  $\text{SiO}_4$  units for single-layered (norbergite), 2-layered (alleghanyite), 3-layered (leucophoenicite) and 4-layered (sonolite) of silicate layers between the brucite layers of humite groups. In particular, the spectrum of four-layered silicate mineral, sonolite shows four individual weak intensity bands at 5285, 5145, 5040 and 5010  $\text{cm}^{-1}$  (1892, 1944, 1984 and 1996 nm) (1.89, 1.94, 1.98 and 2.00  $\mu\text{m}$ ) and three-layered, leucophoenicite at 5410, 5285 and 5180 and 5010  $\text{cm}^{-1}$  (1848, 1892, 1931 and 1996 nm) (1.85, 1.89, 1.93 and 2.00  $\mu\text{m}$ ) suggest the contribution of weak intensity bands by OH-stretching vibrations of hydroxyl groups.

*The 4600 to 4000  $\text{cm}^{-1}$  (2174 to 2500 nm) (2.17 to 2.50  $\mu\text{m}$ ) spectral region*

This spectral region results from combination of IR fundamental modes observed in the mid-IR range. Fig. 4 shows four main groups of bands at 4540, 4470, 4335, and 4120  $\text{cm}^{-1}$  (2203, 2237, 2307 and 2427 nm) (2.20, 2.24, 2.31 and 2.43  $\mu\text{m}$ ) for norbergite and a similar series of bands exhibit by Fe-humites. Bands in the range, 4540-4470  $\text{cm}^{-1}$  (2203-2237nm) (2.20-2.24  $\mu\text{m}$ ) in humite minerals are the combination of fundamental bands due to Si-OH bonding [51]. The bands around 4500-4300  $\text{cm}^{-1}$  (2222-2326 nm) (2.22-2.33  $\mu\text{m}$ ) appear due to the combinations of OH stretching and M-OH bending modes, where M may be Mg, Mn, Al and/or Fe [52]. The observation of combination bands in NIR spectra for tourmalines shows bands at 4529, 4454, 4356 and 4238  $\text{cm}^{-1}$  (2208, 2245, 2296 and 2360 nm) (2.21, 2.25, 2.30 and 2.36  $\mu\text{m}$ ) [53]. For the humite mineral group, three bands centred at 4300, 4200 and 4100  $\text{cm}^{-1}$  (2326, 2381 and 2439 nm) (2.33, 2.38 and 2.44  $\mu\text{m}$ ) and same set of bands are displayed by norbergite and alleghanyite with minimal band position differences. Well resolved bands appear in leucophoenicite and sonalite near 4300  $\text{cm}^{-1}$  (2326 nm) (2.33  $\mu\text{m}$ ) band. OH-bending mode is clearly resolved in humites near 756-724  $\text{cm}^{-1}$  (Fig. 7). The second band in the range 4300-4200  $\text{cm}^{-1}$  (2326-2381 nm) (2.33-2.38  $\mu\text{m}$ ) is attributed to MnOH vibrations (combination of OH-stretching and M-OH-bending modes) [52]. The low wavenumber bands near 4100  $\text{cm}^{-1}$  (2439 nm) (2.44  $\mu\text{m}$ ) may be attributed to (Mg/Ca/Zn)OH units. The shift of combination bands of OH-stretching and M-OH bending modes to lower wavenumbers in humite groups shows compositional variation and possible substitutions of  $\text{Mn}^{2+}$ ,  $\text{Fe}^{2+}$ ,  $\text{Zn}^{2+}$ ,  $\text{Ca}^{2+}$  for  $\text{Mg}^{2+}$ .

*3.4. Mid-IR spectroscopy*

The mid-infrared spectra of the humite minerals are subdivided into three regions according to the observed features in their spectra.

- 1) The 3750- 3250  $\text{cm}^{-1}$  region corresponds to OH stretching vibrations
- 2) The 1100-500  $\text{cm}^{-1}$  region corresponds to the various stretching and bending vibrations of  $\text{SiO}_4$  units.

The spectra of OH-stretching region are shown in Fig. 5. The stretching and bending vibrations in the ranges, 1050-800  $\text{cm}^{-1}$  and 750-500  $\text{cm}^{-1}$  are shown in the Fig. 6. The hydrous components of OH and  $\text{SiO}_4$  groups in the mineral structure act as an aid to distinguish the humite group minerals by FTIR spectroscopy. This technique is a rapid one and most sensitive to identify the OH and  $\text{SiO}_4$  groups in minerals. The spectra of the hydroxyl-stretching region of humites are shown in Fig. 5. Norbergite shows two bands at 3581 and 3572  $\text{cm}^{-1}$  whereas the spectrum of alleghanyite shifts to lower wavenumbers with a splitting of the second band and the bands are 3528, 3484, 3495 and 3469  $\text{cm}^{-1}$ . The three-layered leucophoenicite spectrum also moved further to a lower region at 3368, 3344, 3322 and 3284  $\text{cm}^{-1}$ . The OH region of 4-layered becomes complex and more number of bands resolved at 3679, 3642, 3542 and 3465  $\text{cm}^{-1}$  for sonolite. The shift to lower energy of the spectrum might be the cause of cations like, Ca and Zn, besides Mn in sonolite. A set of six modes at 3685, 3650, 3571, 3561, 3411 and 3393  $\text{cm}^{-1}$  have been reported in the OH fundamental stretching region of chondrodite from Keral Khondalite Belt, India [49]. Analysis of IR spectra of Mg-rich chondrodites having cation impurities like Fe, Ti shows various stretching and bending modes of (Mg-O) and ( $\text{SiO}_4$ ) groups. The assignment of the observed vibrational modes for OH-stretching vibrations and  $\text{SiO}_4$  stretching/ bending vibrations in IR-spectra of humite minerals is presented in Table 3 and compared with data reported for chondrodites from different localities: 1) chondrodite from Keral Khondalite Belt, India [49], 2) sample originated from Limecrest Quarry, Newton, New Jersey, U.S.A [54] and the mineral from U.C., Berkeley, U.S.A [55]. The reason for the difference in band positions of the OH stretching vibrations is attributed to the strength of the hydrogen bond formed between the OH units of the brucite-like layer and the adjacent olivine layers. It is clear from their spectra (Fig. 5) the complexity of OH spectrum increases with number of silicate layers in humites. However, IR spectroscopy is able to differentiate the mineral group from 1, 2, 3 or 4-layered of silicates of humite mineral group, norbergite, alleghanyite, leucophoenicite, sonalite by the main OH bands observed at 3581, 3484 and 3322  $\text{cm}^{-1}$  respectively with an exception to 3679  $\text{cm}^{-1}$  in sonolite.

There are several investigations published on hydrous magnesium silicates and analyses present for stretching and bending modes of Mg-O and  $\text{SiO}_4$  groups in the mid-infrared region [54-57]. Number of modes have been detected in the region 1100-500  $\text{cm}^{-1}$  for the various compositions (Fig. 6). All the network modes concerned with  $\text{SiO}_4$  stretching modes observed here in the range 1050-800  $\text{cm}^{-1}$  are comparable with the modes reported in chondrodites (Table 3). Norbergite, a Mg-humite, gives rise to five mode at 1026, 999, 904, 876 and 854  $\text{cm}^{-1}$ . The spectra of all Mn-bearing humites, were observed to have shifted to lower wavenumber. All the samples show a number of peaks on either side of the most intense peak centered near 876  $\text{cm}^{-1}$ . The patterns look alike but show bands with varying intensities and band positions. Thus the main  $\text{SiO}_4$  stretching mode centered near 876  $\text{cm}^{-1}$  (Fig. 6) shows shift to lower wavenumber for Mn-bearing minerals, alleghanyite, leucophoenicite

and sonalite. The spectra leucophoenicite and sonalite which are the minerals with 3 and 4-silicate layers respectively show increased in complexity and overlapping bands. The M-OH deformation modes observed near  $756\text{ cm}^{-1}$  and two weak bands near  $680$  to  $500\text{ cm}^{-1}$  are the most probable result of  $\text{SiO}_4$  bending vibrations and Mn-O vibrations.

#### 4. Conclusions

The study of UV-Vis spectroscopy of humites, reveals the electronic spectra by two samples, alleghanyite and leucophoenicite. It is of surprise to see the absence of Mn-type spectrum in sonolite, even though the representative chemical formula obtained from EDX analysis shows the presence of manganese in the sample and may be accounted for the impurities like cations of Ca and Zn. The loss of the Mn-spectrum for sonolite, looks as if cation impurities like Ca and Zn are responsible ( $\text{Mn}^{2+}_{0.9} \text{Zn}^{2+}_{0.06} \text{Ca}^{2+}_{0.03} (\text{SiO}_4)_4 (\text{OH}_{0.56} \text{F}_{0.44})$ ).

A pair of sharp bands of alleghanyite and leucophoenicite in UV region at around 410 nm ( $24390 \text{ cm}^{-1}$ ) is identified as due to independent crystal-field transitions of  $\text{Mn}^{2+}$  ion and are assigned to  ${}^6\text{A}_{1g}(\text{S}) \rightarrow {}^4\text{A}_{1g}(\text{G})$  and  ${}^6\text{A}_{1g}(\text{S}) \rightarrow {}^4\text{E}_{1g}(\text{G})$  transitions. The observation of splitting ( $300 \text{ cm}^{-1}$ ) (5nm) of the UV band shows with distinguishable energy may be explained by the distortion of octahedral symmetry of the Mn-bearing humites. The shift of combinational bands of OH-stretching and M-OH bending modes to lower wavenumbers in humite group minerals shows compositional variation and possible substitutions of  $\text{Mn}^{2+}$ ,  $\text{Fe}^{2+}$ ,  $\text{Zn}^{2+}$ ,  $\text{Ca}^{2+}$  for  $\text{Mg}^{2+}$ . The humite mineral group is characterised by two OH stretching vibrations over the range  $3680\text{-}3320 \text{ cm}^{-1}$ . A series of  $\text{SiO}_4$  stretching modes displayed over the range,  $1050\text{-}800 \text{ cm}^{-1}$  symmetrically on either side of an intense peak centred near  $876 \text{ cm}^{-1}$  and the complexity of  $\text{SiO}_4$  stretching and bending spectra increases with the number of silicate layers in Mn-bearing humite minerals.

#### Acknowledgments

The financial and infra-structure support of the Queensland University of Technology, Inorganic Materials Research Program is gratefully acknowledged. The Australian Research Council (ARC) is thanked for funding the instrumentation. One of the authors, B. Jagannadha Reddy is grateful to the Queensland University of Technology for the award of a Visiting Fellowship.

## References

- [1] C. Palache, Cambridge. Am. J. Sci. 29 (1910) 177.
- [2] P. Geijer, Geol. For. Forh. 48 (1926) 84.
- [3] W. H. Taylor and J. West, Proc. Roy. Soc. (London) A117 (1927) 517.
- [4] E. S. Larsen, Am. Mineral. 13 (1928) 354.
- [5] E. S. Larsen, L. H. Bauer and H. Berman, Am. Mineral. 13 (1928) 349.
- [6] A. F. Rogers, Am. Mineral. 20 (1935) 25.
- [7] K. Rankama, Bull. comm. geol. Finlande No. 123 (1938) 81.
- [8] H. Strunz, Zeitschrift fuer Kristallographie, Kristallgeometrie, Kristallphysik, Kristallchemie 99 (1938) 513.
- [9] K. Rankama, Am. Mineral. 32 (1947) 146.
- [10] N. W. Jones, Am. Mineral. 54 (1969) 309.
- [11] R. M. Ganiev, Y. A. Kharitonov, V. V. Ilyukhin and N. V. Belov, Doklady Akademii Nauk SSSR 188 (1969) 1281.
- [12] G. V. Gibbs and P. H. Ribbe, Am. Mineral. 54 (1969) 376.
- [13] N. W. Jones, Am. Mineral. 54 (1969) 309.
- [14] N. W. Jones, P. H. Ribbe and G. V. Gibbs, Am. Mineral. 54 (1969) 391.
- [15] G. V. Gibbs, P. H. Ribbe and C. P. Anderson, Am. Mineral. 55 (1970) 1182.
- [16] P. J. Rentzeperis, Z. Kristallogr., Kristallgeometrie, Kristallphys., Kristallchem. 132 (1970) 1.
- [17] Y. K. Egorov-Tismenko, I. P. Deineko, M. A. Simonov and N. V. Belov, Kristallografiya 16 (1971) 1174.
- [18] P. H. Ribbe and G. V. Gibbs, Am. Mineral. 56 (1971) 1153.
- [19] P. J. Rentzeperis, Chimika Chronika 1 (1972) 267.
- [20] E. L. Belokoneva, M. A. Simonov and N. V. Belov, Kristallografiya 18 (1973) 1275.
- [21] K. Robinson, G. V. Gibbs and P. H. Ribbe, Am. Mineral. 58 (1973) 43.
- [22] P. H. Ribbe, G. V. Gibbs and N. W. Jones, Mineralogical Magazine and Journal of the Mineralogical Society (1876-1968) 36 (1968) 966.
- [23] W. B. Simmons, Jr., D. R. Peacor, E. J. Essene and G. A. Winter, Mineralogical Record 12 (1981) 167.
- [24] G. A. Winter, E. J. Essene and D. R. Peacor, Am. Mineral. 68 (1983) 951.
- [25] P. J. Dunn, American Mineralogist 70 (1985) 379.
- [26] J. W. Anthony, R. A. Bideaux, K. W. Bladh and M. C. Nichols, Handbook of Mineralogy Vol.IV. phosphates, arsenates and vanadates, Vol. 4, Mineral Data Publishing, Tucson, Arizona, 2003.
- [27] B. Wunder, Contributions to Mineralogy and Petrology 132 (1998) 111.
- [28] P. H. Ribbe, Reviews in Mineralogy 5 (1980) 231.
- [29] K. B. N. Sarma, B. Madhusudhana, B. J. Reddy, S. Vedanand and G. Srinivasulu, Solid State Communications 78 (1991) 751.
- [30] K. B. N. Sarma, B. J. Reddy and S. V. J. Lakshman, Proceedings of the Nuclear Physics and Solid State Physics Symposium 24 C (1982) 471.
- [31] A. N. Platonov, K. Langer, M. Wildner, E. V. Polshin and S. S. Matsyuk, Zeitschrift fuer Kristallographie 216 (2001) 154.
- [32] L.G. Liu, C.C. Lin and T.P. Mernagh, Eur. J. Mineral. 11 (1999) 1011.
- [33] ] P.H. Ribbe, Reviews in Mineralogy, Vol. 5, Mineralogical Society of America, Washington, D.C., 1982, pp. 231.

- [34] P.J. Rentzeperis, *Z. Kristallogr.* 132 (1970)1.
- [35] O.V. Petersen, J. Bullhorn and P.J. Dunn, *Mineral. Record* 15 (1984) 299.
- [36] C.A. Francis, *Am. Mineral.* 70 (1985) 182.
- [37] S.L. Penfield and C.H. Warren, *Am. J. Sci.* 8 (1899) 339.
- [38] P.B. Moore, *Am. Mineral.* 52 (1967) 1226.
- [39] P.B. Moore, *Am. Mineral.* 55 (1970) 1146.
- [40] T.J. White and B.G. Hyde, *Am. Mineral.* 68 (1983) 1009.
- [41] M. Yoshinaga, *Memoir Faculty of Science, Kyushu University, Series D, Geology* 14 (1963) 1.
- [42] P.J. Dunn, *Am. Mineral.* 70 (1985) 379.
- [43] P.G. Manning, *Can. Mineral.* 9 (1968) 348.
- [44] K.L. Keester and W.B. White, *Papers and Proc. 5th Gen. Meet. Cambridge, England, London: Mineral. Soc.* (1968) 22.
- [45] D.S. McClure, *Chem. Phys.* 39 (1963) 2284.
- [46] B. Jagannadha Reddy and R.L. Frost, *Spectrochim. Acta Part A* 65 (2006) aaaa.
- [47] C.J. Ballhausen, *Introduction to Ligand Field Theory*, Mc-Graw Hill Book Company, New Delhi, 1962.
- [48] H. Keppler, *Am. Mineral.* 77 (1992) 62.
- [49] P.S.R. Prasad, L.P. Sarma, *Am. Mineral.* 89 (2004) 1056.
- [50] P. Yu, R.J. Kirkpatrick, B. Poe, P.F. McMillan, *X. Cong, J. Am. Ceram. Soc.* 82 (1999) 742.
- [51] A.K. Kronenberg, *Reviews in Mineralogy, Vol. 29, Mineralogical Society of America, Washington, D.C., 1994*, pp. 123.
- [52] R.N. Clark, T. King, M. Klefwa, G.A. Swayze, N.J. Vergo, *Geophysical Res. B95* (1990) 12653.
- [53] P.S.R. Prasad, D. S. Sarma, *Gondwana Research* 8 (2005) 265.
- [54] H. Cynn, A.M. Hofmeister, P.C. Burnley, A. Novrotsky, *Phys. Chem. Mineral.* 23 (1996) 361.
- [55] Q. Williams, *Vibrational spectroscopic study of hydrogen in high pressure minerals assemblages*, In Y. Syono and M.M. Manghnani, Eds., *Terra Publishing Company, Tokyo, High Pressure Research: Applications to Earth and Planetary Sciences*, 1992, pp. 289.
- [56] M. Akaogi, S.I. Akimoto, *Phys. Chem. Mineral.* 13 (1986) 161.
- [57] A.M. Hofmeister, H. Cynn, P.C. Burnley, C. Meade, *Am. Mineral.* 84 (1999) 454.

Mineral name	Origin	Ideal formula	Formula calculated from EDX analysis	Silicate layers	Class
Norbergite	Franklin Limestone Quarry, Franklin, Sussex County, New Jersey	$Mg_3(SiO_4)(OH, F)_2$	$Mg_{2.80}Fe_{0.03}Ca_{0.01}(SiO_4)F_{1.19}(OH)_{0.49}$	1	Orthorhombic
Alleghanyite	Hamayokokawa Mine, Tatuno Cho, Nagano Prefecture, Japan	$(Mn^{2+})_5(SiO_4)_2Mg(OH, F)_2$	$Mn_{11.48}(SiO_4)_2(OH, F)_{3.48}$	2	Monoclinic
Leucophoenicite	Parker Shaft, Franklin, Sussex County, New Jersey	$(Mn^{2+})_7(SiO_4)_3(OH)_2$	$Mn_{6.47}Mg_{0.19}Ca_{0.45}(SiO_4)_3(OH)_{2.22}$	3	Monoclinic
Sonalite*	Franklin Limestone quarry, Franklin, Sussex County, New Jersey	$(Mn^{2+})_9(SiO_4)_4(OH, F)_2$	$Mn^{2+}_{0.9}, Zn^{2+}_{0.06}, Ca^{2+}_{0.03}(SiO_4)_4(OH)_{0.56}, F_{0.44}$	4	Monoclinic

\* Formula calculated from the data reported by Dunn [42]

**Table1**  
**Table of Mn-humite and Mg-humite minerals, their formula, number of silicate layers and symmetry class**

Transition	Alleghanyite [Mn <sub>11.48</sub> (SiO <sub>4</sub> ) <sub>2</sub> (OH,F) <sub>3.48</sub> ]		Leucophoenicite [Mn <sub>6.47</sub> Mg <sub>0.19</sub> Ca <sub>0.45</sub> (SiO <sub>4</sub> ) <sub>3</sub> (OH) <sub>2.22</sub> ]		Sursassite (Reported)[46] [Mn <sup>2+</sup> Al <sub>3</sub> (SiO <sub>4</sub> )(Si <sub>2</sub> O <sub>7</sub> )(OH) <sub>3</sub> ]	
	λ (nm)	ν (cm <sup>-1</sup> )	λ (nm)	ν (cm <sup>-1</sup> )	λ (nm)	ν (cm <sup>-1</sup> )
<sup>6</sup> A <sub>1g</sub> (S) → <sup>4</sup> T <sub>1g</sub> (G)	549	18215	558	17920	580	17240
<sup>6</sup> A <sub>1g</sub> (S) → <sup>4</sup> T <sub>1g</sub> (G)					550c	18180c
<sup>6</sup> A <sub>1g</sub> (S) → <sup>4</sup> T <sub>2g</sub> (G)	453	22075	441	22675	515	19420
<sup>6</sup> A <sub>1g</sub> (S) → <sup>4</sup> T <sub>2g</sub> (G)			435sh	22990sh		
<sup>6</sup> A <sub>1g</sub> (S) → <sup>4</sup> A <sub>1g</sub> (G)	413	24210	415	24095	470	21280
<sup>6</sup> A <sub>1g</sub> (S) → <sup>4</sup> E <sub>1g</sub> (G)	408	24510	410	24390	450c	22220c

sh-shoulder; c-component

**Table2**  
Assignment of Mn<sup>2+</sup> bands in Mn-humites and a comparison with Mn-silicate sursassite

Norbergite (Franklin Limestone Quarry, New Jersey) [Present study]	Alleghanyite (Hamayokokawa Mine, Japan) [ Present study]	Leucophoenicite (Parker Shaft, New Jersey) [Present study]	Sonalite ( Franklin Limestone quarry, New Jersey) Present study [Present study]	Chondrodite (Kerala Khondalite Belt, India) [49]	Chondrodite (Limecrest Quarry, New Jersey, U.S.A.) [54]	Chondrodite (U.C., Berkeley, U.S.A.) [ 55]	Assignment
3581	3528		3679	3692	3687	3690	Hydroxyl stretch
3572	3495		3642sh	3674		3662	Hydroxyl stretch
	3484			3571			Hydroxyl stretch
	3469sh		3465	3412	3568	3568	Hydroxyl stretch
					3559	3560	Hydroxyl stretch
		3368		3412			Hydroxyl stretch
		3344c		3392c			
		3322			3385	3382	Hydroxyl stretch
		3284sh					
1026	1050	1022					SiO <sub>4</sub> -asymmetric stretch
999	958	970	983	997	987	994	SiO <sub>4</sub> -asymmetric stretch
904	890	945	903sh	961	955	955	SiO <sub>4</sub> -asymmetric stretch
		912sh					
876	863	863	867	887	891	892	SiO <sub>4</sub> -asymmetric stretch
854	850		825	847	850	851	SiO <sub>4</sub> -asymmetric stretch
	825	809	804				SiO <sub>4</sub> -asymmetric stretch
	797sh						
756	724	744	745	754	761	757	M-OH deformation
				745sh	748sh		
626	669	658	604	613	619	618	SiO <sub>4</sub> -asymmetric bend/MgO <sub>6</sub>

560	563	572	585				motion
		541		534	541	551	MO stretching vibrations (M = Fe/Mn/Ca/Zn)
				494	489		MO stretching vibrations (M = Fe/Mn/Ca/Zn)
							MOH deformation vibrations (M = Fe/Mn/Ca/Zn)
					440		MOH vibrations (M = Fe/Mn/Ca/Zn)
				420	418		MOH vibrations (M = Fe/Mn/Ca/Zn)
					397		MOH vibrations (M = Fe/Mn/Ca/Zn)

sh-shoulder; c-component

**Table 3**  
**Assignments of the observed IR modes ( $\text{cm}^{-1}$ ) for different humite minerals.**

### *List of Tables*

**Table1**

**Table of Mn-humite and Mg-humite minerals, their formula, number of silicate layers and symmetry class**

**Table2**

**Assignment of Mn<sup>2+</sup> bands in Mn-humites and a comparison with Mn-silicate sursasite**

**Table 3**

**Assignments of the observed IR modes (cm<sup>-1</sup>) for different humite minerals.**

### *List of figures*

**Fig. 1. UV-Vis reflectance spectra of alleghanyite and leucophoenicite in the 400 to 650 nm region.**

**Fig. 2. NIR reflectance spectra of norbergite, alleghanyite, leucophoenicite and sonolite in the 7400 to 6400 cm<sup>-1</sup> region**

**Fig. 3. NIR reflectance spectra of norbergite, alleghanyite, leucophoenicite and sonolite in the 5650 to 4650 cm<sup>-1</sup> region**

**Fig. 4. NIR reflectance spectra of norbergite, alleghanyite, leucophoenicite and sonolite in the 4600 to 4000 cm<sup>-1</sup> region**

**Fig. 5. IR reflectance spectra of norbergite, alleghanyite, leucophoenicite and sonolite in the 3750 to 3250 cm<sup>-1</sup> region**

**Fig. 6. IR reflectance spectra of norbergite, alleghanyite, leucophoenicite and sonolite in the 1100 to 500 cm<sup>-1</sup> region**

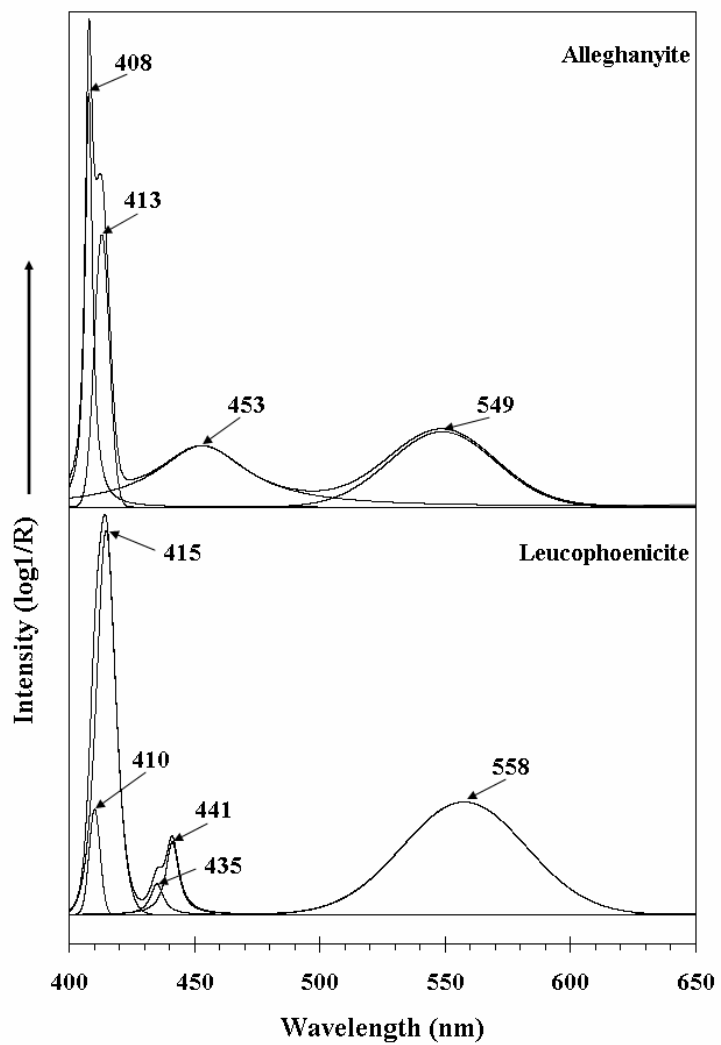


**Figure 1**

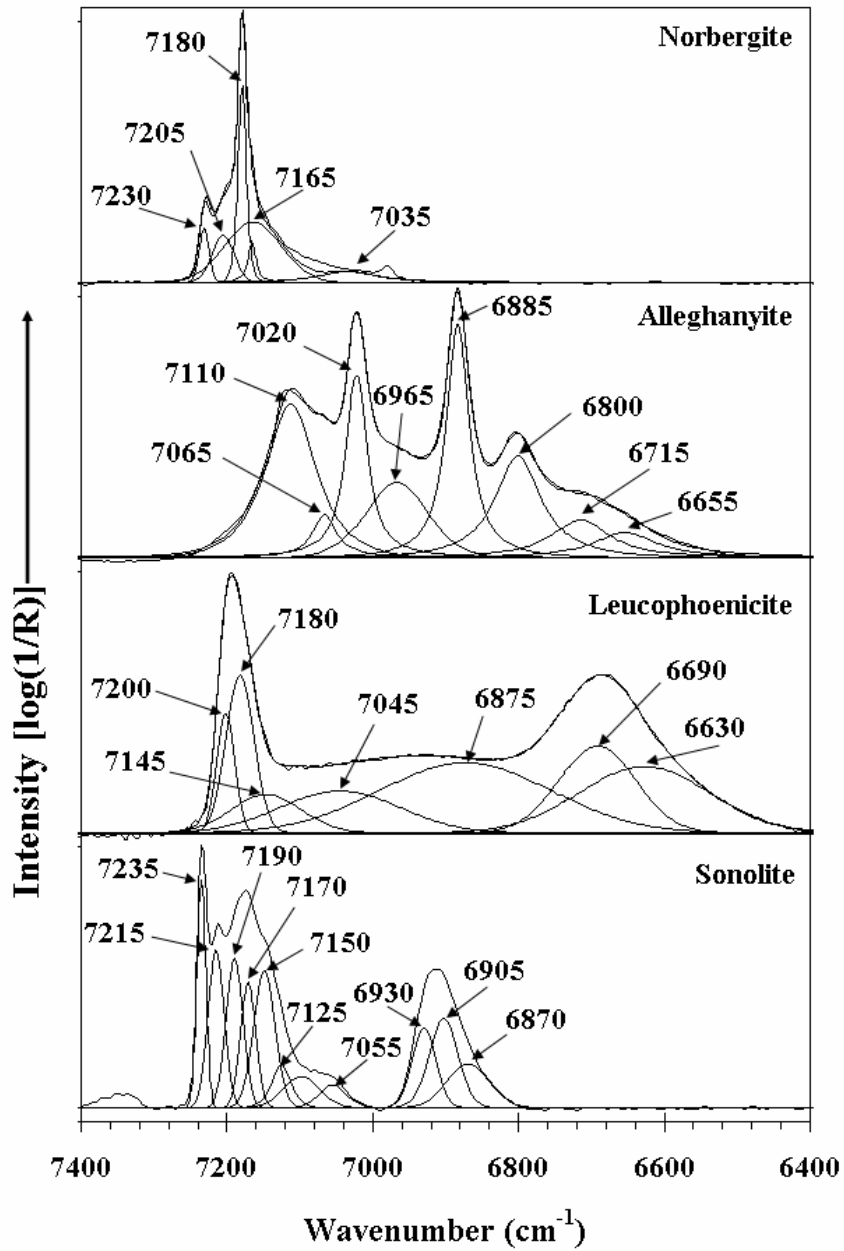


Figure 2

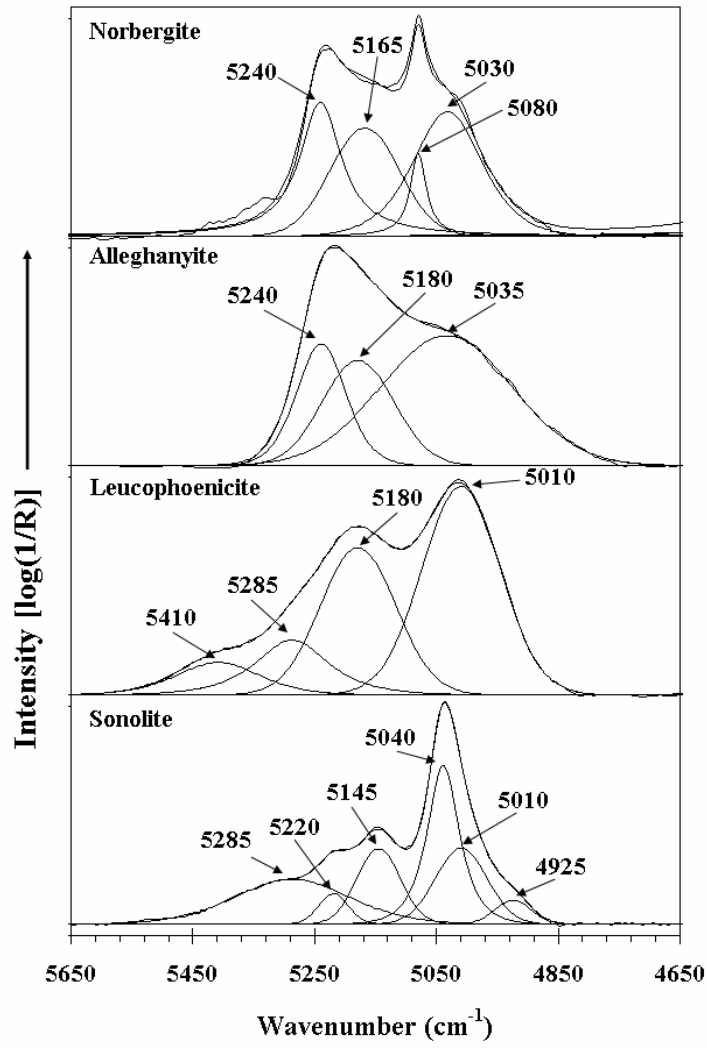


Figure 3

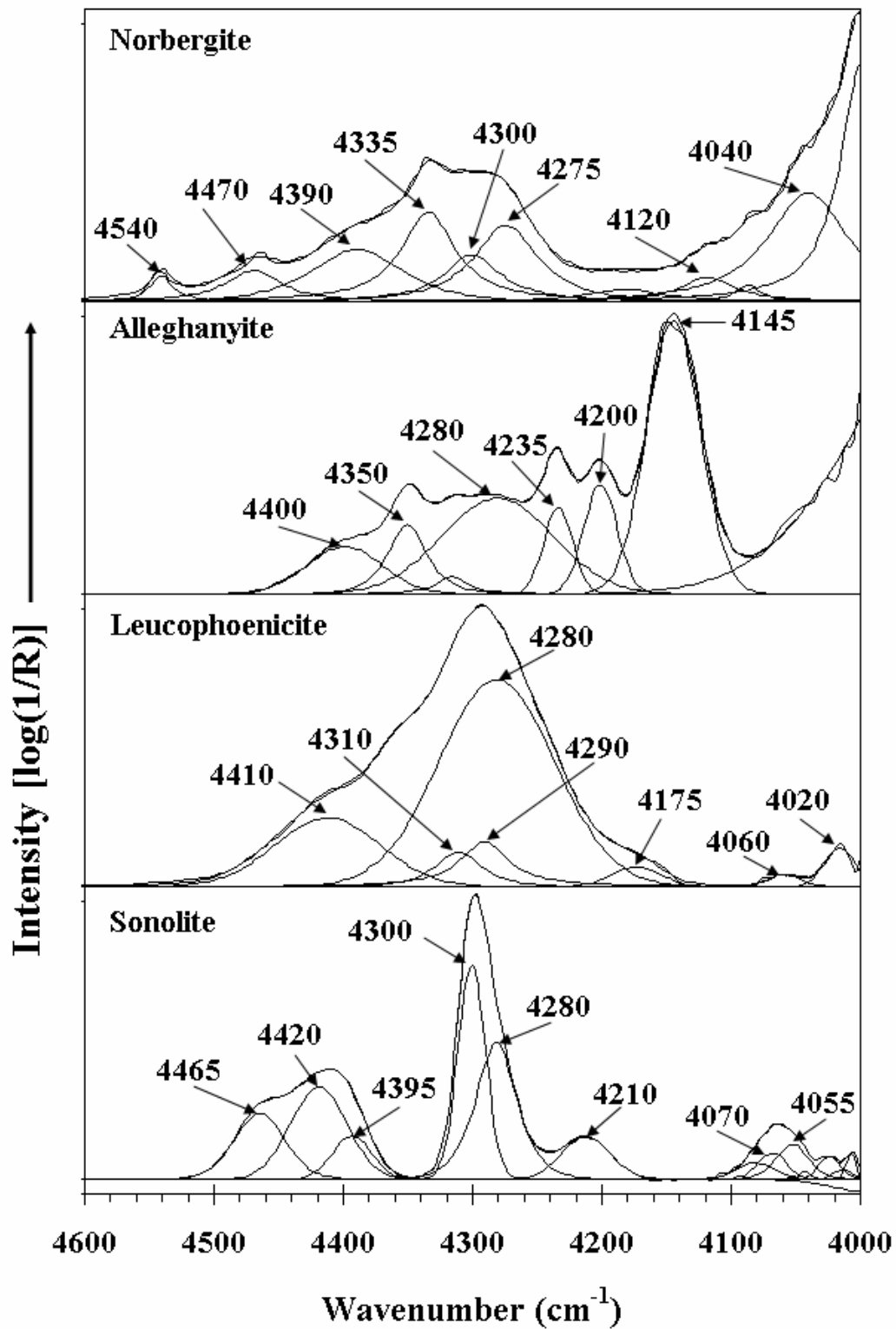


Figure 4

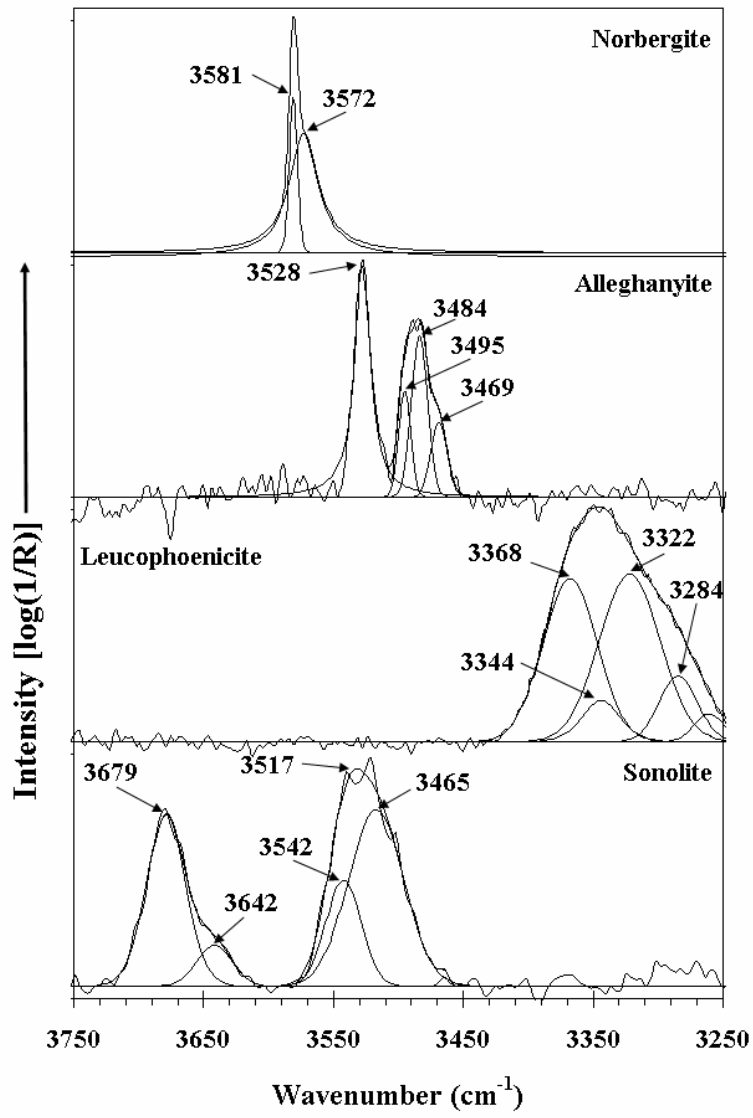


Figure 5

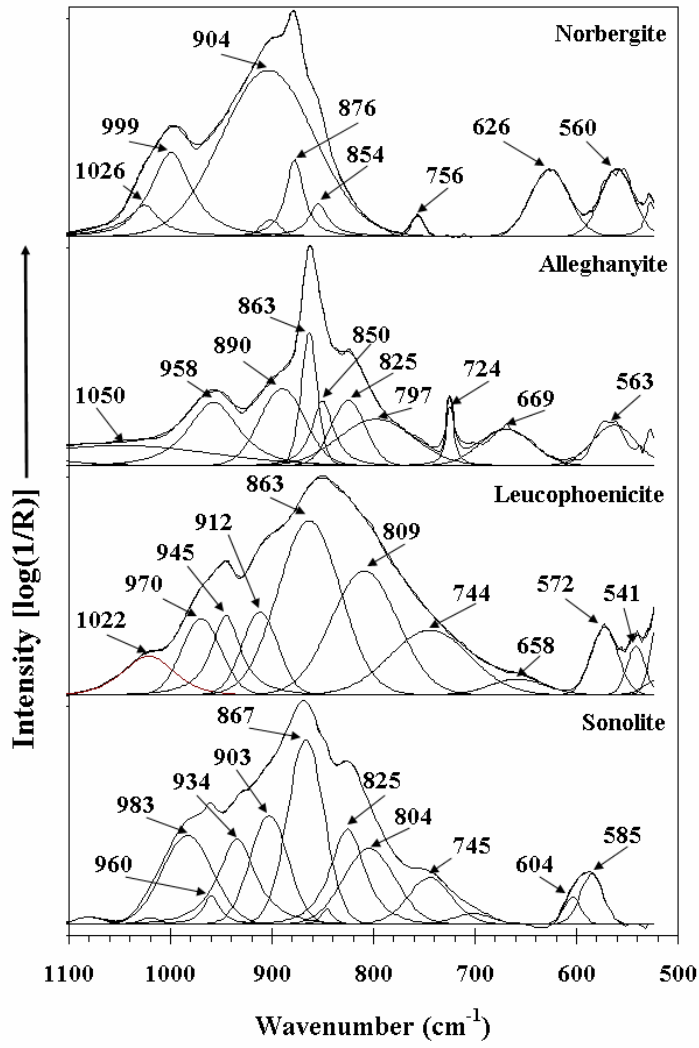


Figure 6